Since January 2020 Elsevier has created a COVID-19 resource centre with free information in English and Mandarin on the novel coronavirus COVID-19. The COVID-19 resource centre is hosted on Elsevier Connect, the company's public news and information website.

Infection, Genetics and Evolution 93 (2021) 104923

Contents lists available at ScienceDirect

Infection, Genetics and Evolution

journal homepage: www.elsevier.com/locate/meegid

Research paper

Differential host circRNA expression profiles in human lung epithelial cells infected with SARS-CoV-2

Mengmei Yang [a,1], Mengdi Qi [a,b,1], Liangzi Xu [a,1], Pu Huang [a,1], Xu Wang [a], Jing Sun [a], Jiandong Shi [a,*], Yunzhang Hu [a,*]

[a] Yunnan Provincial Key Laboratory of Vector-borne Diseases Control and Research, Institute of Medical Biology, Chinese Academy of Medical Sciences and Peking Union Medical College, Kunming, Yunnan, China
[b] Kunming Medical University, Kunming, Yunnan, China

ARTICLE INFO

Keywords:
SARS-CoV-2
COVID-19
RNA-seq
Lung epithelial cells
Circular RNA

ABSTRACT

Severe acute respiratory syndrome coronavirus 2 (SARS-CoV-2) is an emerging and highly pathogenic coronavirus that causes coronavirus disease (COVID-19), and might even lead to death. Circular RNAs (circRNAs), a new type of RNAs, are implicated in viral pathogenesis and host immune responses. However, their dynamic expression patterns and functions during SARS-CoV-2 infection remain to be unclear. We herein performed genome-wide dynamic analysis of circRNAs in human lung epithelial cells infected with SARS-CoV-2 at four time points. A total of 6118 circRNAs were identified at different genomic locations, including 5641 known and 477 novel circRNAs. Notably, a total of 42 circRNAs were significantly dysregulated, wherein 17 were up-regulated and 25 were down-regulated following infection at multiple phases. The gene ontology and KEGG enrichment analyses revealed that the parental genes of circRNAs were mainly involved in immune and inflammatory responses. Further, the RNA binding protein (RBP) prediction analysis indicated that the dysregulated circRNAs could regulate mRNA stability, immunity, cell death by binding specific proteins. Additionally, the circRNA-miRNA-gene network analysis showed that circRNAs indirectly regulated gene expression by absorbing their targeted miRNAs. Collectively, these results shed light on the roles of circRNAs in virus-host interactions, facilitating future studies on SARS-CoV-2 infection and pathogenesis.

1. Introduction

Severe acute respiratory syndrome coronavirus 2 (SARS-CoV-2) is a novel and highly infectious coronavirus that belong to the Betacoronavirus genus, and can lead to coronavirus disease (COVID-19) (Gorbalenya et al., 2013; Lu et al., 2020a; Zhou et al., 2020). SARS-CoV-2 infection causes flu-like symptoms, including fever, cough, and dyspnea, which can later progress to acute respiratory distress syndrome (ARDS), pneumonia, renal failure, and even death (Chen et al., 2020; Wang et al., 2020). Since the outbreak of SARS-CoV-2 in December 2019, the epidemic has spread to more than 200 countries around the world, which led to nearly 100 million infections and more than 2 million deaths (WHO, 2021). SARS-CoV-2 infects several human tissues and organs through skin and mucous membrane by broad tissue tropism of it. The virus is internalized into the cell by angiotensin-converting enzyme 2 (ACE2) and TMPRSS2 (Shulla et al., 2011; Ziegler et al., 2020). After its entry into the alveolar epithelial cells, SARS-CoV-2 replicates rapidly and triggers a strong inflammatory as well as immune responses, resulting in cytokine storm syndrome (Hadjadj et al., 2020; Liu et al., 2020). Thus, understanding the infection and pathogenesis of SARS-CoV-2 are necessary for treating COVID-19 disease.

To decode the host immune response as well as the pathogenesis of SARS-CoV-2, there were only few studies conducted on transcriptomics, proteomics and metabonomics of cell cultures infected with SARS-CoV-2, as well as the patient materials (Appelberg et al., 2020; Bojkova et al., 2020; Bruzzone et al., 2020; Fagone et al., 2020; Sun et al., 2020; Vishnubalaji et al., 2020; Xiong et al., 2020). Previous studies have highlighted the characteristics of viral infection, which lacked robust induction of type I and type III interferons, and instead released numerous chemokines and excessive cytokines. Additionally, in vivo analysis of antiviral host transcriptional response showed that SARS-CoV-2 induced a strong antiviral response by activating antiviral

* Corresponding authors.
E-mail addresses: shijiandong@imbcams.com.cn (J. Shi), huyunzhangym@126.com (Y. Hu).
[1] These authors contributed equally to this work.

https://doi.org/10.1016/j.meegid.2021.104923
Received 6 April 2021; Received in revised form 11 May 2021; Accepted 13 May 2021
Available online 15 May 2021

factors such as OAS1–3 and IFIT1–3 and T helper type 1 (Th1) chemokines CXCL9/10/11, along with a reduction in the transcription of ribosomal proteins (Lieberman et al., 2020). Although these studies have revealed the characteristics of the host antiviral transcriptional response of SARS-CoV-2 infection in cell cultures and tissue samples of COVID-19 patients, understanding of non-coding RNAs, especially the circRNA transcriptional dynamics and functions of the host during SARS-CoV-2 infection still remains to be unclear.

Circular RNAs (circRNAs) are a new class of closed circular RNAs that are produced from their parental genes by back-splicing (Memczak et al., 2013). CircRNAs, which are a class of gene regulators, are involved in a variety of physiological and pathological processes, including growth, development, metastasis and other diseases (Du et al., 2017; Du et al., 2016; Liang et al., 2017). Mounting evidence has shown that circRNAs also play an important regulatory role in viral infection and subsequent host antiviral responses (Tan and Lim, 2020). As competitive endogenous RNAs, they also play a regulatory role by acting as microRNA (miRNA) sponges (Hansen et al., 2013). They can bind to RNA-associated proteins to form RNA protein complexes, which in turn regulate gene transcription (Li et al., 2015). On theone hand, viral infection can change the expression profile of circRNAs in the host cells. Several circRNAs were aberrantly modulated during HIV infection (Zhang et al., 2018) and in human cytomegalovirus (Deng et al., 2021). CircRNA regulates antiviral immunity by competitively binding with NF90/NF110 (Li et al., 2017). Liu et al. have shown that endogenous circRNAs are globally degraded to release protein kinase (PKR) after viral infection, which in turn is activated to aid in innate immune response (Liu et al., 2019). On the other hand, the genome of many viruses can induce circRNAs to regulate viral infections and pathogenesis, including Epstein-Barr virus (EBV) (Qiao et al., 2019), Kaposi's sarcoma herpesvirus (KSHV) (Tagawa et al., 2018), hepatitis B virus (HBV) (Sekiba et al., 2018), and human papilloma virus (HPV) (Zhao et al., 2019). According to a recent study, circRNAs encoded by SARS-CoV-2 down-regulated genes showed association with metabolic processes of cholesterol, alcohol, fatty acid, while up-regulated genes showed association with cellular responses to oxidative stress (Cai et al., 2021). However, a comprehensive genome-wide host circRNA dynamic expression and function during SARS-CoV-2 infection still remains to be unclear.

Therefore, to gain better understanding on the molecular basis of COVID-19, the dynamic expression and potential functions of circRNAs in human lung epithelial Calu-3 cells infected with SARS-CoV-2 at four time points were investigated. The results from this study showed that the host circRNA expression profiles were dynamically changed during SARS-CoV-2 infection. Furthermore, some candidate circRNAs that might function in SARS-CoV-2 infection were revealed. Collectively, our results provided insights on the roles of circRNAs in virus-host interactions, and facilitated conduction of studies on SARS-CoV-2 infection and pathogenesis in the future.

2. Materials and methods

2.1. Data processing and circRNA prediction

RNA-seq datasets (Sun et al., 2020) of SARS-CoV-2 infected Calu-3 cells were downloaded from the National Genomics Data Center (https://bigd.big.ac.cn/) with accession number PRJCA002617, with 3 replicates for each experiment. The raw reads were filtered to obtain clean reads by removing the adapter sequences, N-bases and low-quality reads with Trimmomatic (0.36) (Bolger et al., 2014). To ensure the reliability of the reads obtained, quality inspections were conducted through faspP software (Chen et al., 2018). The clean reads were mapped to the human GRCh38 reference genome using Hisat2 (2.2.1.0) (Kim et al., 2015). All unmapped reads were further used for predicting and identifying circRNAs using CIRI (v2.0.3) (Gao et al., 2015) based on junction reads and GT-AG splicing signals. The reads mapped to each gene were counted by htseq-count (Anders et al., 2015), and the obtained circRNA candidates were compared with that of the circAtlas (Ji et al., 2019) (http://159.226.67.237:8080/new/index.php) and circBase databases (Glažar et al., 2014) (http://circrna.org/cgi-bin/singlerecord.cgi?id=mmu_circ_0001771) to determine the known and novel circRNAs. Data processing and analysis were assisted by Shanghai OE Biotech (Shanghai, China).

2.2. Differential analysis of circRNAs

The expression levels of circRNAs were quantified by mapping the back-splicing junction reads per million mapped reads (RPM). The R package DESEq. (1.18.0) (Burden et al., 2014) was applied to standardize the number of junction reads of circRNAs in each sample. DESeq software was used to estimate the differential expression of circRNAs. Differentially expressed circRNAs were selected based on the following criteria: $|\log2 \text{ fold change}| \geq 1$ and P-value < 0.05. Following RPM analysis, principal component analysis (PCA) was performed to investigate the correlation of the samples.

2.3. Validation of circRNAs by qRT-PCR

To verify the expression of circRNAs, 8 differential circRNAs were selected from cells infected with SARS-CoV-2 at 24hpi. The human bronchial epithelial cells (BEAS-2B), which is a model of human respiratory disease, were infected with SARS-CoV-2 at multiplicity of infection (MOI) of 1 for 24 h. All experiments were performed in the high-level biosafety facility of the National Kunming High-level Biosafety Primate Research Center under Biosafety Level 3 (BSL-3) conditions. SARS-CoV-2 was obtained from the National Kunming High-level Biosafety Primate Research Center, China. At 24 h post infection (hpi), the cells were harvested and the total RNA was extracted to obtain cDNA by reverse transcription-PCR using GoScript Reverse Transcription System (Promega, USA) according to the manufacturer's protocol. Next, quantitative real-time polymerase chain reaction (qRT-PCR) was used to quantify the relative expression level of dysregulated circRNAs in CFX96 Touch Real-Time PCR Detection System (BioRad, Berkeley, USA) by using 2 × TSINGKE Master qPCR Mix (Beijing, China). The cycling parameters of qPCR reaction were as follows: 95 °C for 10 min, 40 cycles at 95 °C for 15 s, 55 °C for 15 s, and 72 °C for 30s, and finally, 65 °C to 95 °C, with an increment of 0.5 °C/5 s for analyzing the melting curve to determine the specificity of qPCR. The divergent primers of circRNAs for qPCR were in Supplementary Table 1. Each group included three independent samples and assessed in triplicate. The $2^{-\Delta\Delta Ct}$ method (Livak and Schmittgen, 2001) was used to compare the relative expression fold changes of SARS-CoV-2 infected versus mock-mocked group with Human *GAPDH* gene (glyceraldehyde-3-phosphate dehydrogenase) as a reference gene.

2.4. GO and KEGG pathway analysis

Gene Ontology (GO) and the Kyoto Encyclopedia of Genes and Genomes (KEGG) (Kanehisa et al., 2008) functional enrichment analyses were carried with GOseq package to predict the function of parental genes that correspond to the differentially expressed circRNAs. GO (http://www.geneontology.org/) analysis was done to annotate the genes under the category of cellular component, biological process and molecular function. The number of differential circRNAs included in each GO term was counted, and the hypergeometric distribution test method was used to calculate the significance of enrichment of differential circRNAs in each GO term. KEGG pathway enrichment using hypergeometric test was used to predict the involvement of cellular pathways for parental genes of dysregulated circRNAs. The pathways of GO and KEGG with corrected P-values of less than 0.05 were considered as significantly enriched.

2.5. RNA binding protein (RBP) prediction of circRNAs

As a protein sponge, circRNAs can bind to RNA-associated proteins to form RNA-protein complexes that regulate gene transcription (Li et al., 2015). The RBPs that bind the differential circRNAs were predicted by using the CircInteractome web tool (https://omictools.com/circinteractome-tool) (Dudekula et al., 2016).

2.6. Construction of competing endogenous RNA (ceRNA) network

The top 6 significantly dysregulated circRNAs (such as hsa_circ_0080941, hsa_circ_0080942, hsa_circ_0067985, hsa_circ_0005630, hsa_circ_0001681 and hsa_circ_0060927) and the top 20 significantly up-regulated and the top 20 down-regulated genes were selected to establish the ceRNA network (Supplementary Table 2). Firstly, the interaction between miRNAs and the 6 circRNAs were analyzed using miRanda (v3.3a) (John et al., 2004) to construct a circRNA–miRNA network. Secondly, the miRNA–gene network was constructed in the same way. Finally, the integrated circRNA–miRNA–gene regulatory network was constructed and visualized using Cytoscape (3.0) (Su et al., 2014).

3. Results

3.1. Identification and characteristics of circRNAs in SARS-CoV-2-infected and uninfected lung epithelial cells

In this study, the whole transcriptome datasets (Sun et al., 2020) of SARS-CoV-2 infected Calu-3 cells comprised a total of 298.92 G clean data across 24 samples at four time points. The distribution of effective data for these samples was 9.25–15.64 G, and the average GC content was 41.88%. The comparison rate was 86.21–92.63% for these datasets by comparing them to a human reference genome. The quality control of all samples was assessed by PCA based on normalized counts from DESeq2, and this indicated that high quality was achieved if majority of the samples were well clustered (Fig. 1A). Based on CIRI analysis, a total

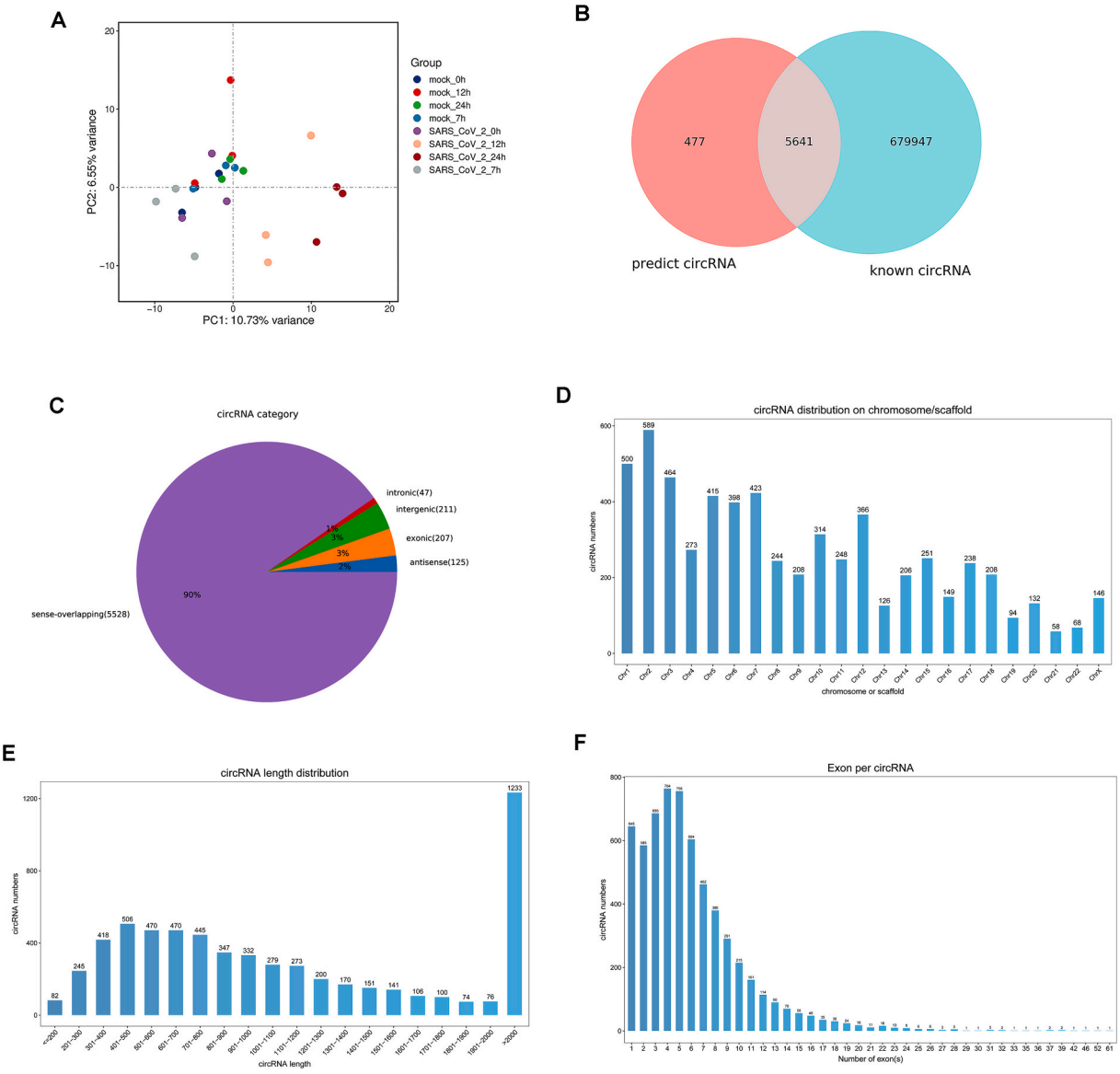

Fig. 1. Identification and characterization of circRNAs in human lung epithelial Calu-3 cells. (A) Principal component analysis (PCA) plot of the expressed circRNAs. (B) The comparison of all identified circRNAs with circBase database to identify known and novel circRNAs. (C) The genomic category distribution of circRNAs. (D) The number distribution of the identified circRNAsacross human chromosomes (E) The length distributionof the identified circRNAs. (F) The number of exons in each identified circRNA sequence.

number of 6118 distinct host circRNAs in mock-infected and SARS-CoV-2-infected Calu-3 lung epithelial cells were identified (Supplementary Table 3). Among them, a total of 5641 known and 477 novel circRNAs were distinguished by comparing the predicted results with circBase and circAtlas database (Fig. 1B). To describe the characteristics of circRNAs, the distribution in gene position, chromosome distribution, length, exon number, and GC content for all circRNAs were analyzed. The results with regard to position distribution of circRNAs on genome showed that the circRNAs were classified into 5 categories, including sense-overlapping circRNAs (90.36%), exonic circRNAs (3.38%), intergenic circRNAs (3.45%), antisense circRNAs (2.04%) and intronic circRNAs (0.77%). The vast majority of circRNAs were sense-overlapping, while a small portion was either intergenic or intronic (Fig. 1C), and this is consistent with the results reported in the previous studies (Deng et al., 2021; Lu et al., 2020b). Generally, the transcription of host circRNAs in human cells remains diverse. By analyzing the genomic position of the parent genes of circRNAs, the host circRNAs were shown to be widely transcribed throughout the whole genome across all chromosomes, except the Y chromosome (Fig. 1D). The distribution number of circRNAs on chromosome 2 was the most frequently transcribed, reaching 589, while that on chromosome 21 was the least, only 58. The distribution of circRNA sequence lengths showed that most of the circRNAs sequences ranged from 200 nt to 1000 nt (Fig. 1E). The average circRNA length was 3436.36 nt, with a maximum of 98,623 nt, and a minimum of 58 nt. Most of the circRNAs were observed to be shorter than 2000 nt, and the number of circRNAs was decreased with increasing sequence length after 700 nt. The distribution of the number of exons in circRNA sequences was shown in figure (Fig. 1F.), and most of the identified circRNAs consisted of four or five exons. The GC content distribution of circRNA sequences was calculated, and found that the GC content of the circRNAs ranged from 30% to 60% (Supplementary Fig. 1). Collectively, these results from the whole transcriptome datasets (Sun et al., 2020) of SARS-CoV-2 infected Calu-3 cells showed that the host circRNAs were widely and abundantly expressed by back-splicing in human lung epithelial cells, suggesting their potential regulatory roles in response to SARS-CoV-2 infection.

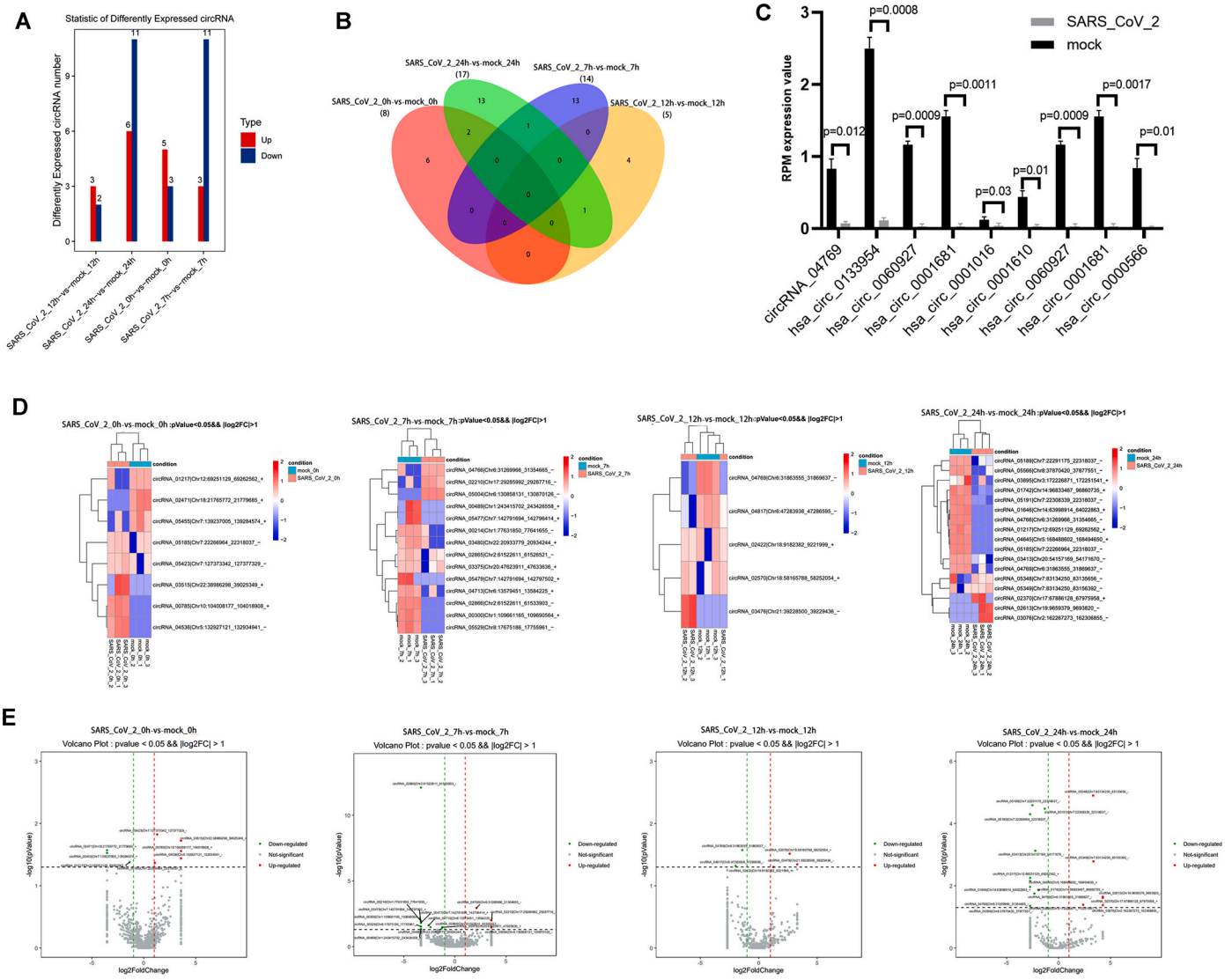

Fig. 2. Dynamic expression profiles of circRNAs during SARS-CoV-2 infection across four time points. (A) Statistical histogram of the differentially expressed circRNAs. (B) Venn diagram of the differentially expressed circRNAs across four time points. The horizontal axis is log2foldchange and the Y axis is - log10Pvalue. (C) Expression change of some highly abundant circRNAs detected in two or more samples quantified by PRM value. (D) Hierarchical cluster heat maps of differentially expressed circRNAs across four time points. "red color" represents up-regulation, and "blue color"represents down-regulation. (E) The volcano plot of the differently expressed circRNAs. The grey dots denote non-significantly expressed circRNAs. The up-regulated circRNAs are presented as red dots and the down-regulated circRNAs are presented as blue dots.

3.2. Dysregulated circRNA expression profiles in SARS-CoV-2-infected lung epithelial cells

Next, to elucidate the overall and dynamic changes of host circRNAs expression along with the progression of SARS-CoV-2 infection, a sequential infection experiment was conducted in Calu-3 cells at four time points (0, 7, 12, and 24 hpi) (Sun et al., 2020). Based on the whole transcriptome datasets (Sun et al., 2020) of SARS-CoV-2 infected Calu-3 cells and the screening criteria of differential expression analysis, a total of 42 significantly dysregulated circRNAs were identified during SARS-CoV-2 infection (Supplementary Table 4). More specifically, there were a total of 5 up-regulated and 3 down-regulated circRNAs at 0hpi, 3 up-regulated and 11 down-regulated circRNAs at 7 hpi, 3 up-regulated and 2 down-regulated circRNAs at 12 hpi, 6 up-regulated and 11 down-regulated circRNAs at 24 hpi, respectively (Fig. 2A). The differentially repeated circRNAs were also removed at different time points. Interestingly, with the progression of infection, the differential expression of circRNAs was gradually increased. However, the expression of circRNAs was sharply decreased at 12hpi, and then rebounded to the highest number at 24hpi later. But the common differential expression of circRNAs at four time points was not observed (Fig. 2B), which might be due to dynamic regulation of expression and function of circRNAs. Notably, some circRNAs have showed a higher degree of differential change in RPM expression value when compared with others, such as hsa_circ_0133954, hsa_circ_0060927, hsa_circ_0001681, hsa_circ_0001016, and hsa_circ_0060927, suggesting their involvement in the regulation of virus infection (Fig. 2C). Furthermore, heat maps were generated to illustrate the clustering expression trend of dysregulated circRNAs at four time points (Fig. 2D). Furthermore, the volcano plots were drawn to show the overall distribution of differentially expressed circRNAs (Fig. 2E). Taken together, the above results indicated that the host circRNA expression profiles were dynamically changed during SARS-CoV-2 infection, suggesting the complex molecular behavior of the host cells to virus infection.

3.3. Validation of circRNA expression pattern by qRT-PCR

Based on whole transcriptome datasets (Sun et al., 2020) of SARS-CoV-2 infected Calu-3 cells, we screened out 42 significantly dysregulated circRNAs during SARS-CoV-2 infection. To validate the high consistency or universality of these expression changes of circRNAs in human lung epithelial cells, another human bronchial epithelial cells (BEAS-2B) were used to verify the expression changes of circRNAs during SARS-CoV-2 infection. A total of 8 significantly dysregulated circRNAs, including hsa_circ_0000566, hsa_circ_0060927, hsa_circ_0067985, circRNA_04769, hsa_circ_0001681, hsa_circ_0080941, hsa_circ_0080942, hsa_circ_0005630, were selected to verify the change in expression in response to SARS-CoV-2 infection by qRT-PCR experiments. As shown in Fig. 3, the expression patterns of 7 circRNAs are similar to those of RNA-seq, supporting the reliability of the quantitative expression of circRNAs of RNA-seq. These results suggested the high consistency or universality of these expression changes of circRNAs in human lung epithelial cells during SARS-CoV-2 infection.

3.4. Function associated analysis of circRNA parental genes

To further delineate the potential biological function of dysregulated circRNAs during SARS-CoV-2 infection, the GO and KEGG function enrichment analysis was conducted for parental genes of the dysregulated circRNAs. Overall, the parental genes are mainly enriched in biological process and cellular component, while the molecular function is rarely enriched at four time points. The enrichment analysis at 0 hpi suggested that the parental genes of differentially expressed circRNAs were implicated with biological processes, including signal transduction (GO:0023014), defense response to virus (GO:0051607), regulation of apoptotic process (GO:0042981), and innate immune response (GO:0045087), mRNA binding (GO:0003729), mRNA processing (GO:0006397), endocytosis (GO:0006897) etc. (Fig. 4A and Supplementary Table 5). The parental genes of differentially expressed circRNAs at 7 hpi showed association with type I interferon signaling pathway (GO:0060337), antigen processing and presentation of exogenous peptide antigen via MHC class I (GO:0002480), regulation of immune response (GO:0050776), interferon-gamma-mediated signaling pathway (GO:0060333), etc. (Fig. 4B and Supplementary Table 5). The parental genes of differentially expressed circRNAs at 12 hpi showed association with interleukin-7-mediated signaling pathway (GO:0038111), humoral immune response (GO:0006959), adaptive immune response (GO:0002250), immune response (GO:0006955), inflammatory response (GO:0006954), etc. (Fig. 4C and Supplementary Table 5). The parental genes of differentially expressed circRNAs at 24 hpi showed association with detection of virus (GO:0009597), regulation of type III interferon production (GO:0034344), positive regulation of interferon-beta secretion (GO:0035549), cytoplasmic pattern recognition receptor signaling pathway in response to virus (GO:0039528), antigen processing and presentation of exogenous peptide antigen via MHC class I, etc. (Fig. 4D and Supplementary Table 5). Some common biological processes, such as regulation of immune response and defense response to virus, were enriched at four time points during viral infection.

Next, the pathways that were significantly enriched by parental genes of differential circRNAs in lung epithelial cells during SARS-CoV-2infection were further analyzed. At 0 hpi, only a few pathways showed significant enrichment, including mRNA surveillance pathway (hsa03015), Rap1 signaling pathway (hsa04015) and Ras signaling pathway (hsa04014) (Fig. 5A and Supplementary Table 6). During the early stage of virus infection (7 hpi), a large number of pathways showed significant enrichment in antigen processing and presentation (hsa04612), Fc gamma R-mediated phagocytosis (hsa04666),

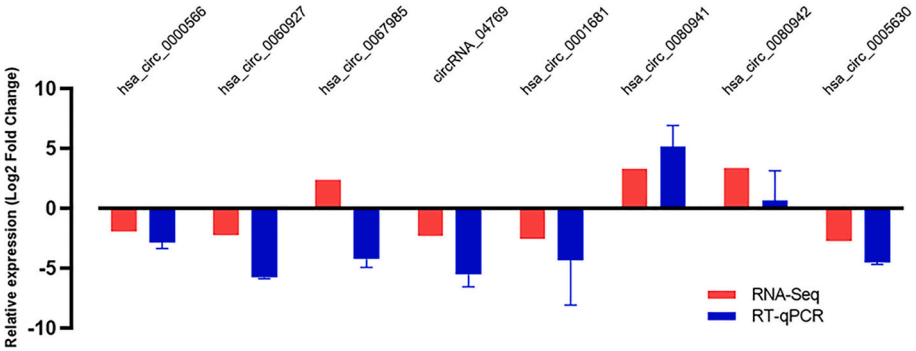

Fig. 3. Validation of the RNA-seq data using qRT-PCR. The relative expression levels of circRNAs measured in SARS-CoV-2-infected or mock-infected BEAS-2B cells. Data are expressed as mean ± SD from at least two independent experiments. The vertical axis shows the mean fold change.

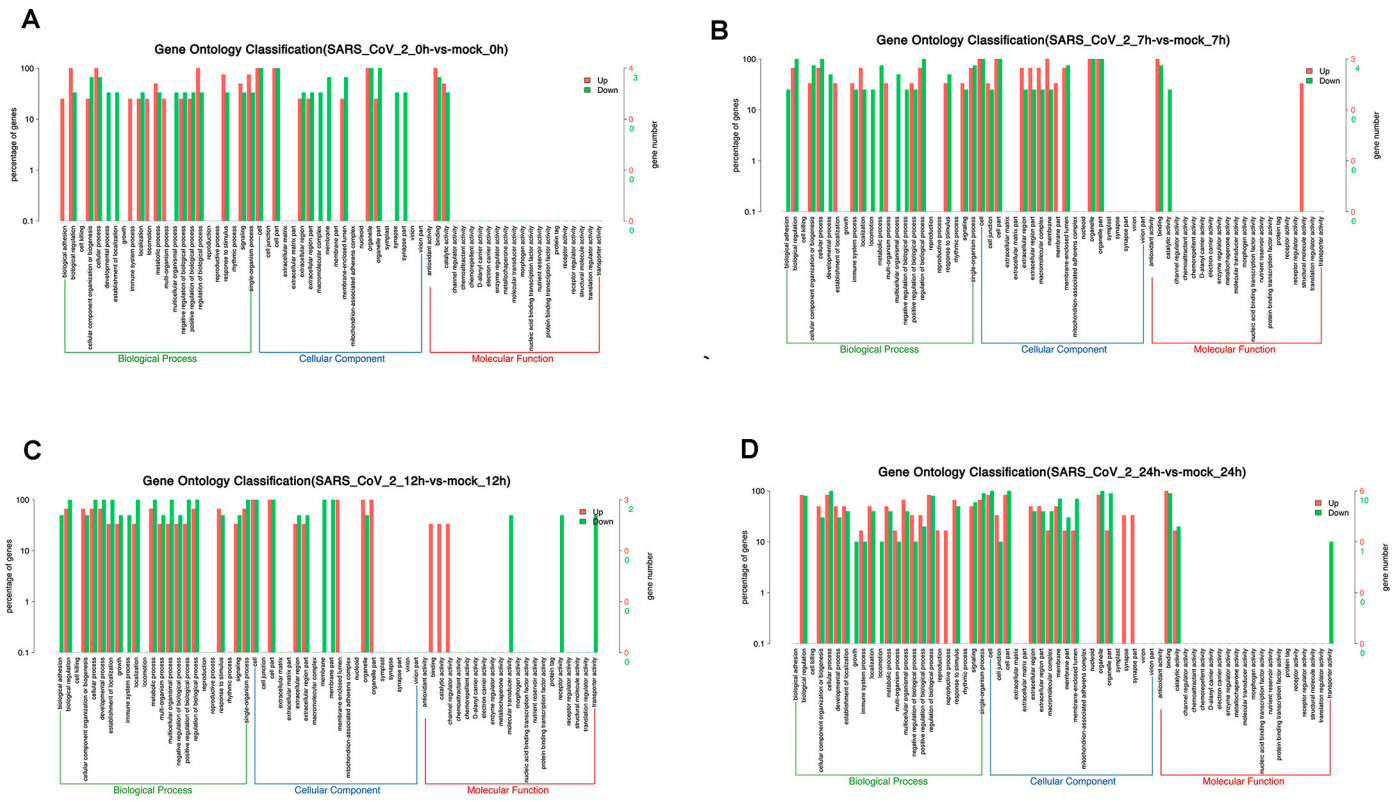

Fig. 4. GO enrichment analysis of the parental genes of differentially expressed circRNAs in SARS-Cov-2_0 hpi vs. control (A), SARS-Cov-2_7 hpi vs. control (B), SARS-Cov-2_12 hpi vs. Control (C), and SARS-Cov-2_24 hpi vs. Control (D).

chemokine signaling pathway (hsa04062), and MAPK signaling pathway (hsa04010) (Fig. 5B and Supplementary Table6). At 12 hpi, a few signaling pathways were significantly enriched in the cytokine-cytokine receptor interaction (hsa04060), ubiquitin mediated proteolysis (hsa04120) and endocytosis (hsa04144) (Fig. 5C and Supplementary Table 6). Finally, in the late stage of virus infection (24 hpi), a few signaling pathways were significantly enriched in RIG-I-like receptor signaling pathway (hsa04622), antigen processing and presentation (hsa04612), natural killer cell mediated cytotoxicity (hsa04650), and mRNA surveillance pathway (hsa03015) (Fig. 5D and Supplementary Table 6). Notably, these GO and KEGG enrichment analyses results were similar to those reported by other studies (Li et al., 2021; Lou et al., 2019). Overall, these findings indicated that the parental genes of these differentially expressed circRNAs are involved in the regulation of viral infection and host antiviral response.

3.5. Functional analysis of circRNA regulating virus-host interaction by acting as miRNA and protein sponges

As a competitive miRNA or protein sponge, circRNAs play an important role in regulating gene expression and function (Hansen et al., 2013; Li et al., 2015). To further explore the potential functions of circRNAs during SARS-CoV-2 infection, an integrated analysis of circRNA-miRNA-gene network was carried out. The top six significantly dysregulated circRNAs and top 40 significantly dysregulated genes during SARS-CoV-2 infection were used to construct ceRNA regulatory network. The results showed that the top 3 up-regulated circRNAs showed indirect up-regulation of the expression of the protein coding genes by binding their targeted miRNAs (Fig. 6A). Similarly, the top 3 down-regulated circRNAs showed indirect down-regulation of the expression of the protein coding genes by binding their targeted miRNAs (Fig. 6B and Supplementary Table 7). These results suggested that the circRNAs can form a complex regulatory network with a variety of RNAs at transcriptional level to regulate gene expression in response to viral infection. Furthermore, a large number of RBPs that bind to circRNAs were obtained by using the CircInteractome web tool (Table 1). The predicted binding relationship between circRNA and protein showed that the regulation characteristics of one for many and many for one. Among these, one circRNA can bind to one or multiple RBPs, and one RBP can be bind to either one or multiple circRNAs. Furthermore, functional enrichment analysis of RBPs showed that most of the RBPs, such as EIF4A3, AGO2, TIAL1, IGF2BP3, LIN28B and FUS, were implicated in biological processes, including RNA stability, translation, regulation of cell apoptotic process and immunity. Notably, these analyses only provide some candidate proteins that circRNAs may bind from the perspective of bioinformatics, and more experimental evidence is needed to determine the interactions between circRNAs and RBPs. Collectively, these results suggested that these circRNAs in the network interaction of circRNA-miRNA-gene network might play a functional role in antiviral transcriptional response of the host cells during SARS-CoV-2 infection.

4. Discussion

In this study, the RNA-seq data from SARS-CoV-2 infected human lung epithelial cells were analyzed at four time points to characterize the circRNA transcriptional dynamics of the host response. This is the first study to systematically report the expression profiles of circRNAs in SARS-CoV-2 infected human lung epithelial cells. A total of 6118 circRNAs were identified from diverse genomic locations, while 42 significantly dysregulated circRNAs were obtained at four time points. Our results demonstrated that SARS-CoV-2 infection significantly impacted the circRNA expression profiles of the host, suggesting their potential biological function during virus infection.

Recently, some transcriptomic and proteomic studies of SARS-CoV-2 infected cells in vitro also revealed multiple key genes, proteins and

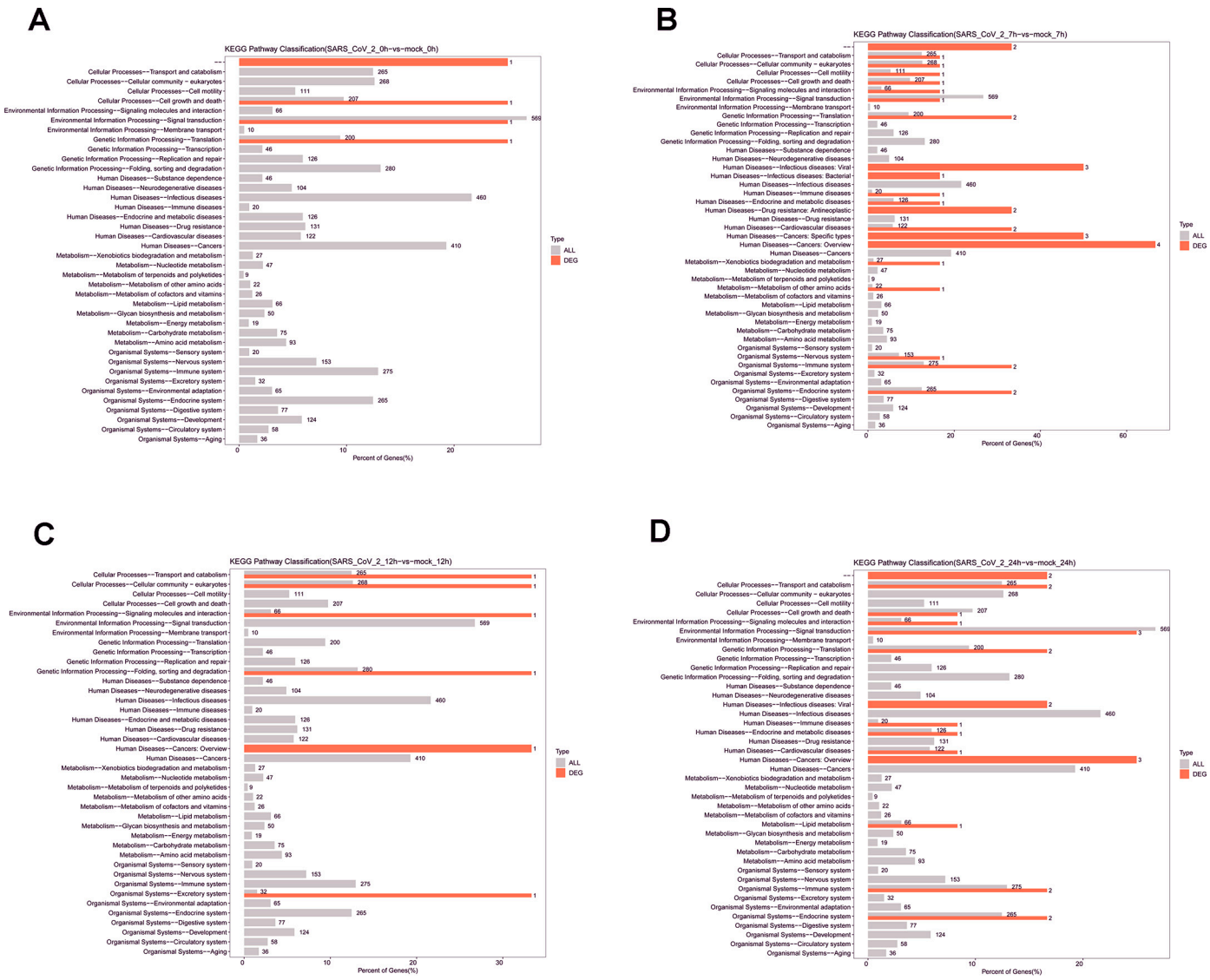

Fig. 5. KEGG enrichment analysis of the parental genes of all and the differential circRNAs in SARS-Cov-2_0 hpi vs. control (A), SARS-Cov-2_7 hpi vs. control (B), SARS-Cov-2_12 hpi vs. Control (C), and SARS-Cov-2_24 hpi vs. Control (D).

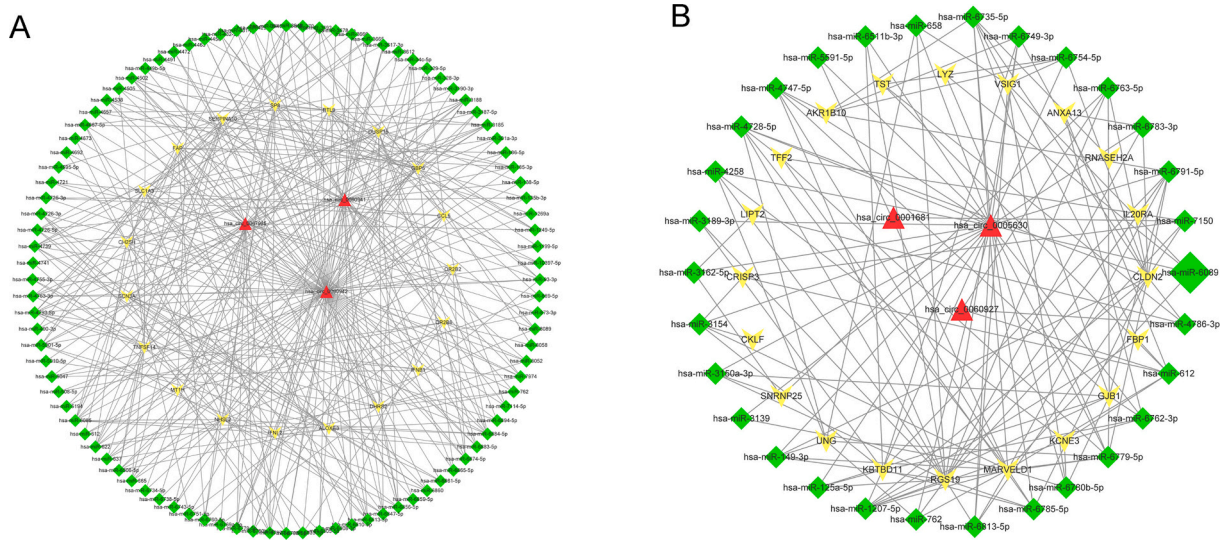

Fig. 6. ceRNA networks between differentially expressed circRNAs and genes in response to SARS-CoV-2 infection.

Table 1
RBPs binding to the dysregulated circRNAs during SARS-CoV-2 infection.

Dysregulated circRNAs	Parental Gene	RBP
hsa_circ_0000259	SKL	AGO2, EIF4A3, FIMRP, HuR, IGF2BP3, U2AF65
hsa_circ_0073904	AFF4	AUF1, EIF4A3, FUS, HuR, IGF2BP3
hsa_circ_0079557	RAPGEF5	EIF4A3
hsa_circ_0082096	ZNF800	AGO2, AUF1, C22ORF28, EIF4A3, EWSR, FMRP, FXR2, HuR, IGF2BP3, LIN28B, PUM2, TIAL1, ZC3H7B
hsa_circ_0000417	CPSF6	EIF4A3, HuR, IGF2BP3, PUM2, TDP43, TIA1, TIAL1, U2AF65
hsa_circ_0000835	MIB1	AUF1, EIF4A3, FUS, TDP43
hsa_circ_0133519	UBN2	AGO2, EIF4A3, FUS, HuR, IGF2BP2, PTB, U2AF65
hsa_circ_0106467	NUFIP2	AGO2, EIF4A3, HNRNPC, IGF2BP2, PUM2, U2AF65, ZC3H7B
hsa_circ_0114166	ZZZ3	AGO2, DGCR8, EIF4A3, FUS, HNRNPC, HuR, IGF2BP3, TIAL1, U2AF65
hsa_circ_0110400	GSTM4	EIF4A3
hsa_circ_0017241	SDCCAG8	EIF4A3
hsa_circ_0001016	XPO1	EIF4A3, HNRNPC, HuR, IGF2BP3
hsa_circ_0001017	XPO1	AUF1, EIF4A3, HNRNPC, HuR, IGF2BP3, U2AF65, ZC3H7B
hsa_circ_0001165	NCOA3	EIF4A3, FMRP, IGF2BP1, IGF2BP3, U2AF65
hsa_circ_0001206	CRKL	EIF4A3, TDP43
hsa_circ_0007218	SIRT5	AGO2, EIF4A3, PTB
hsa_circ_0000826	ANKRD12	EIF4A3
hsa_circ_0108703	NEDD4L	AGO2, EIF4A3, PTB, TDP43
hsa_circ_0001195	BRWD1	AGO2, EIF4A3
hsa_circ_0001610	TNFRSF21	EIF4A3
hsa_circ_0107544	BPTF	AGO2, EIF4A3, IGF2BP3, TAF15
hsa_circ_0067985	FNDC3B	EIF4A3, HuR
hsa_circ_0080941	PCLO	EIF4A3
hsa_circ_0080942	PCLO	EIF4A3, FUS
hsa_circ_0102377	SYNE2	EIF4A3, EWSR1, FUS, U2AF65
hsa_circ_0000566	VRK1	AGO2, EIF4A3, HuR, U2AF65
hsa_circ_0001550	RARS	AGO2, DGCR8, EIF4A3, HuR, U2AF65
hsa_circ_0079557	RAPGEF5	EIF4A3
hsa_circ_0133954	RAPGEF5	EIF4A3
hsa_circ_0005630	RAB11FIP1	EIF4A3
hsa_circ_0001681	RAPGEF5	EIF4A3,FUS

signaling pathways that are activated by virus infection (Bojkova et al., 2020; Fagone et al., 2020). The transcriptomic data from primary normal human bronchial epithelial cells (NHBE) showed that SARS-CoV-2 infection activates antiviral interferon (IFN) innate response. Several interferon stimulating genes, acute inflammatory response and tumor necrosis factor (TNF) were significantly activated during virus infection (Fagone et al., 2020). An integrative proteo-transcriptomic analysis that identified ErbB, HIF-1, mTOR and TNF signaling pathways showed marked modulation during SARS-CoV-2 infection (Appelberg et al., 2020). Consistent with these results, a large number of parental genes of differential circRNAs enriched in those pathways were associated with antiviral interferon (IFN) response, chemokine signaling pathway, and MAPK signaling pathway and RIG-I-like receptor signaling pathway. These results suggested that the genes related to early inflammatory response, immune response, and cell signal transduction act as parental genes of circRNAs and play biological functions during SARS-CoV-2 infection. It is worth noting that the differential expression of circRNAs was gradually increased with progression of infection. However, the expression of circRNAs was decreased sharply at 12hpi, and then rebounded to the highest number at 24hpi later. Not only that, the common differential expression of circRNAs at four time points was not observed, which might be due to the dynamic regulation of expression and function of circRNAs. These results suggested complex molecular behavior of the host cells in response to viral infection.

The parental genes of dysregulated circRNAs were analyzed by GO and KEGG analyses to better understand their potential roles. The GO and KEGG analyses indicated that main processes such as immune responses, chemokine signaling pathway, MAPK signaling pathway, RIG-I-like receptor signaling pathway and signaling transduction were significantly enriched during SARS-CoV-2 infection. The parental genes of dysregulated circRNAs showed enrichment in immune function and defense to viral infection in the early stages (0 and 7 hpi) in SARS-CoV-2 infected Calu-3 cells, implying early inflammatory response, and this is consistent with the results reported from Sun's study (Sun et al., 2020). In the late time point of infection (12–24 hpi), the parental genes of dysregulated circRNAs were widely enriched in regulating type III interferon production, positive regulation of interferon-beta secretion, antigen processing and presentation of exogenous peptide antigen.

It has been reported that circRNAs play a regulatory role by binding with RBPs.

in mammals (Hentze et al., 2018). Thus, the Circ interactome web tool was utilized to predict the RBPs of differential circRNAs. The results showed that one circRNA can sponge to multiple proteins, and those RBPs are implicated in a variety of biological processes and possesses varied physical functions. Many RBPs are related to RNA stability. Other RBPs, such as AGO2, EIF4A3 and IGF2BP3 are related to translation (Nielsen et al., 1999), and FMRP is related to cellular response to virus (Zhou et al., 2014). Specifically, the PUM2 protein can sponge to 3 circRNAs, which is positively regulated to RIG-I signaling pathway (Narita et al., 2014). In this study, TDP43, which is a kind of RBP, was also predicted to regulate the apoptotic process of the host cell (Ayala et al., 2008). RBPs prediction is consistent with the results of GO and KEGG enrichment analyses. These analyses provide new evidence to further study the functioning of differential circRNAs. Additionally, the interaction analysis between differential circRNAs and genes mediated by miRNAs showed that circRNA act as miRNA sponges, thereby modulating the binding of miRNA to target genes.

In summary, this study described the host circRNA transcriptional dynamics at four time points in SARS-CoV-2 infected human lung epithelial cells. Some differentially expressed circRNAs, important KEGG pathways that are related to viral infection, inflammatory response and the immune response were identified. These findings provide new insights into circRNA expression and function, and greatly improve our understanding with regard to the pathogenesis of SARS-CoV-2 and host antiviral responses.

The following are the supplementary data related to this article.

Declaration of Competing Interest

The authors declare that they have no competing interests.

Acknowledgements

We sincerely thank professor Taijiao Jiang, who is from Center for Systems Medicine, Institute of Basic Medical Sciences, Chinese Academy of Medical Sciences & Peking Union Medical College, for providing RNA-seq datasets of SARS-CoV-2 infected Calu-3 cells with accession number PRJCA002617. This study was supported by the Applied Basic Research Key Project of Yunnan (CN) (202001AS070046), the Chinese Academy of Medical Sciences (CAMS) Innovation Fund for Medical Sciences (2017-I2M-3-022), the Yunnan Technology Innovation Talent Projects (2017HB096), and the Fund for Reserve Talents of Young and Middle-aged Academic and Technical Leaders of Yunnan Province (2019HB043).

Appendix A. Supplementary data

Supplementary data to this article can be found online at https://doi.org/10.1016/j.meegid.2021.104923.

References

Anders, S., Pyl, P.T., Huber, W., 2015. HTSeq–a Python framework to work with high-throughput sequencing data. Bioinformatics. 31 (2), 166–169.

Appelberg, S., Gupta, S., Svensson Akusjärvi, S., et al., 2020. Dysregulation in Akt/mTOR/HIF-1 signaling identified by proteo-transcriptomics of SARS-CoV-2 infected cells. Emerg. Microb. Infect. 9 (1), 1748–1760.

Ayala, Y.M., Misteli, T., Baralle, F.E., 2008. TDP-43 regulates retinoblastoma protein phosphorylation through the repression of cyclin-dependent kinase 6 expression. Proc. Natl. Acad. Sci. U. S. A. 105 (10), 3785–3789.

Bojkova, D., Klann, K., Koch, B., et al., 2020. Proteomics of SARS-CoV-2-infected host cells reveals therapy targets. Nature. 583 (7816), 469–472.

Bolger, A.M., Lohse, M., Usadel, B., 2014. Trimmomatic: a flexible trimmer for Illumina sequence data. Bioinformatics. 30 (15), 2114–2120.

Bruzzone, C., Bizkarguenaga, M., Gil-Redondo, R., et al., 2020. SARS-CoV-2 infection Dysregulates the Metabolomic and Lipidomic profiles of serum. iScience 23 (10), 101645.

Burden, C.J., Qureshi, S.E., Wilson, S.R., 2014. Error estimates for the analysis of differential expression from RNA-seq count data. PeerJ. 2, e576.

Cai, Z., Lu, C., He, J., et al., 2021. Identification and characterization of circRNAs encoded by MERS-CoV, SARS-CoV-1 and SARS-CoV-2. Brief. Bioinform. 22 (2), 1297–1308.

Chen, N., Zhou, M., Dong, X., et al., 2020. Epidemiological and clinical characteristics of 99 cases of 2019 novel coronavirus pneumonia in Wuhan, China: a descriptive study. Lancet. 395 (10223), 507–513.

Chen, S., Zhou, Y., Chen, Y., et al., 2018. Fastp: an ultra-fast all-in-one FASTQ preprocessor. Bioinformatics. 34 (17), i884–i890.

Deng, J., Huang, Y., Wang, Q., et al., 2021. Human cytomegalovirus influences host circRNA transcriptions during productive infection. Virol. Sin. 36 (2), 241–253.

Du, W.W., Yang, W., Liu, E., et al., 2016. Foxo3 circular RNA retards cell cycle progression via forming ternary complexes with p21 and CDK2. Nucleic Acids Res. 44 (6), 2846–2858.

Du, W.W., Fang, L., Yang, W., et al., 2017. Induction of tumor apoptosis through a circular RNA enhancing Foxo3 activity. Cell Death Differ. 24 (2), 357–370.

Dudekula, D.B., Panda, A.C., Grammatikakis, I., et al., 2016. CircInteractome: a web tool for exploring circular RNAs and their interacting proteins and microRNAs. RNA Biol. 13 (1), 34–42.

Fagone, P., Ciurleo, R., Lombardo, S.D., et al., 2020. Transcriptional landscape of SARS-CoV-2 infection dismantles pathogenic pathways activated by the virus, proposes unique sex-specific differences and predicts tailored therapeutic strategies. Autoimmun. Rev. 19 (7), 102571.

Gao, Y., Wang, J., Zhao, F., 2015. CIRI: an efficient and unbiased algorithm for de novo circular RNA identification. Genome Biol. 16 (1), 4.

Glažar, P., Papavasileiou, P., Rajewsky, N., 2014. circBase: a database for circular RNAs. RNA. 20 (11), 1666–1670.

Gorbalenya, A.E., Baker, S.C., Baric, R.S., et al., 2013. The species severe acute respiratory syndrome-related coronavirus: classifying 2019-nCoV and naming it SARS-CoV-2. Nat. Microbiol. 5, 536–544.

Hadjadj, J., Yatim, N., Barnabei, L., et al., 2020. Impaired type I interferon activity and inflammatory responses in severe COVID-19 patients. Science. 369 (6504), 718–724.

Hansen, T.B., Jensen, T.I., Clausen, B.H., et al., 2013. Natural RNA circles function as efficient microRNA sponges. Nature. 495 (7441), 384–388.

Hentze, M.W., Castello, A., Schwarzl, T., et al., 2018. A brave new world of RNA-binding proteins. Nat. Rev. Mol. Cell Biol. 19 (5), 327–341.

Ji, P., Wu, W., Chen, S., et al., 2019. Expanded expression landscape and prioritization of circular RNAs in mammals. Cell Rep. 26 (12), 3444-3460.e3445.

John, B., Enright, A.J., Aravin, A., et al., 2004. Human MicroRNA targets. PLoS Biol. 2 (11), e363.

Kanehisa, M., Araki, M., Goto, S., et al., 2008. KEGG for linking genomes to life and the environment. Nucleic Acids Res. 36 (Database issue), D480–D484.

Kim, D., Langmead, B., Salzberg, S.L., 2015. HISAT: a fast spliced aligner with low memory requirements. Nat. Methods 12 (4), 357–360.

Li, H., Tang, W., Jin, Y., et al., 2021. Differential CircRNA expression profiles in PK-15 cells infected with Pseudorabies virus type II. Virol. Sin. 36 (1), 75–84.

Li, X., Liu, C.X., Xue, W., et al., 2017. Coordinated circRNA biogenesis and function with NF90/NF110 in viral infection. Mol. Cell 67 (2), 214-227.e217.

Li, Z., Huang, C., Bao, C., et al., 2015. Exon-intron circular RNAs regulate transcription in the nucleus. Nat. Struct. Mol. Biol. 22 (3), 256–264.

Liang, H.F., Zhang, X.Z., Liu, B.G., et al., 2017. Circular RNA circ-ABCB10 promotes breast cancer proliferation and progression through sponging miR-1271. Am. J. Cancer Res. 7 (7), 1566–1576.

Lieberman, N.A.P., Peddu, V., Xie, H., et al., 2020. In vivo antiviral host transcriptional response to SARS-CoV-2 by viral load, sex, and age. PLoS Biol. 18 (9), e3000849.

Liu, C.X., Li, X., Nan, F., et al., 2019. Structure and degradation of circular RNAs regulate PKR activation in innate immunity. Cell 177 (4), 865-880.e821.

Liu, J., Li, S., Liu, J., et al., 2020. Longitudinal characteristics of lymphocyte responses and cytokine profiles in the peripheral blood of SARS-CoV-2 infected patients. EBioMedicine. 55, 102763.

Livak, K.J., Schmittgen, T.D., 2001. Analysis of relative gene expression data using real-time quantitative PCR and the 2(-Delta Delta C(T)) method. Methods. 25 (4), 402–408.

Lou, Y.Y., Wang, Q.D., Lu, Y.T., et al., 2019. Differential circRNA expression profiles in latent human cytomegalovirus infection and validation using clinical samples. Physiol. Genomics 51 (2), 51–58.

Lu, R., Zhao, X., Li, J., et al., 2020a. Genomic characterisation and epidemiology of 2019 novel coronavirus: implications for virus origins and receptor binding. Lancet. 395 (10224), 565–574.

Lu, S., Zhu, N., Guo, W., et al., 2020b. RNA-Seq revealed a circular RNA-microRNA-mRNA regulatory network in Hantaan virus infection. Front. Cell. Infect. Microbiol. 10, 97.

Memczak, S., Jens, M., Elefsinioti, A., et al., 2013. Circular RNAs are a large class of animal RNAs with regulatory potency. Nature. 495 (7441), 333–338.

Narita, R., Takahasi, K., Murakami, E., et al., 2014. A novel function of human Pumilio proteins in cytoplasmic sensing of viral infection. PLoS Pathog. 10 (10), e1004417.

Nielsen, J., Christiansen, J., Lykke-Andersen, et al., 1999. A family of insulin-like growth factor II mRNA-binding proteins represses translation in late development. Mol. Cell. Biol. 19 (2), 1262–1270.

Qiao, Y., Zhao, X., Liu, J., et al., 2019. Epstein-Barr virus circRNAome as host miRNA sponge regulates virus infection, cell cycle, and oncogenesis. Bioengineered. 10 (1), 593–603.

Sekiba, K., Otsuka, M., Ohno, M., et al., 2018. DHX9 regulates production of hepatitis B virus-derived circular RNA and viral protein levels. Oncotarget. 9 (30), 20953–20964.

Shulla, A., Heald-Sargent, T., Subramanya, G., et al., 2011. A transmembrane serine protease is linked to the severe acute respiratory syndrome coronavirus receptor and activates virus entry. J. Virol. 85 (2), 873–882.

Su, G., Morris, J.H., Demchak, B., et al., 2014. Biological network exploration with Cytoscape 3. Curr. Protoc. Bioinformatics 47, 8.13.1–8.13.24.

Sun, J., Ye, F., Wu, A., et al., 2020. Comparative Transcriptome analysis reveals the intensive early stage responses of host cells to SARS-CoV-2 infection. Front. Microbiol. 11, 593857.

Tagawa, T., Gao, S., Koparde, V.N., et al., 2018. Discovery of Kaposi's sarcoma herpesvirus-encoded circular RNAs and a human antiviral circular RNA. Proc. Natl. Acad. Sci. U. S. A. 115 (50), 12805–12810.

Tan, K.E., Lim, Y.Y., 2020. Viruses join the circular RNA world. FEBS J. https://doi.org/10.1111/febs.15639. Advance online publication.

Vishnubalaji, R., Shaath, H., Alajez, N.M., 2020. Protein coding and long noncoding RNA (lncRNA) transcriptional landscape in SARS-CoV-2 infected bronchial epithelial cells highlight a role for interferon and inflammatory response. Genes 11 (7), 760.

Wang, D., Hu, B., Hu, C., et al., 2020. Clinical characteristics of 138 hospitalized patients with 2019 novel coronavirus-infected pneumonia in Wuhan, China. JAMA. 323 (11), 1061–1069.

WHO Coronavirus Disease (COVID-19) Dashboard, 2021. Available at: https://www.who.int/.

Xiong, Y., Liu, Y., Cao, L., et al., 2020. Transcriptomic characteristics of bronchoalveolar lavage fluid and peripheral blood mononuclear cells in COVID-19 patients. Emerg. Microb. Infect. 9 (1), 761–770.

Zhang, Y., Zhang, H., An, M., et al., 2018. Crosstalk in competing endogenous RNA networks reveals new circular RNAs involved in the pathogenesis of early HIV infection. J. Transl. Med. 16 (1), 332.

Zhao, J., Lee, E.E., Kim, J., et al., 2019. Transforming activity of an oncoprotein-encoding circular RNA from human papillomavirus. Nat. Commun. 10 (1), 2300.

Zhou, P., Yang, X.L., Wang, X.G., et al., 2020. A pneumonia outbreak associated with a new coronavirus of probable bat origin. Nature. 579 (7798), 270–273.

Zhou, Z., Cao, M., Guo, Y., et al., 2014. Fragile X mental retardation protein stimulates ribonucleoprotein assembly of influenza a virus. Nat. Commun. 5, 3259.

Ziegler, C.G.K., Allon, S.J., Nyquist, S.K., et al., 2020. SARS-CoV-2 receptor ACE2 is an interferon-stimulated gene in human airway epithelial cells and is detected in specific cell subsets across tissues. Cell 181 (5), 1016-1035.e1019.